

**Deliverable Report for Grant Agreement Number 760813****Deliverable 1.4****Report on experimental determination of the (long-term) fate of ENM  
in advanced lung, GIT and liver cell models (M30)****Due date of deliverable: 30/06/2020****Actual submission date: 30/09/2020****Lead beneficiary for this deliverable: AMI**

<b>Dissemination Level:</b>		
PU	Public	
PP	Restricted to other programme participants (including the Commission Services)	
RE	Restricted to a group specified by the consortium (including the Commission Services)	
CO	Confidential, only for members of the consortium (including the Commission Services)	X

## TABLE OF CONTENTS

<b>1. DESCRIPTION OF TASK</b>	<b>3</b>
<b>2. DESCRIPTION OF WORK &amp; MAIN ACHIEVEMENTS</b>	<b>4</b>
2.1 Experimental part	5
2.1.1 Cell cultures	5
2.1.2 ENM Materials	6
2.1.3 ENM Sample	6
2.1.4 Short- and long-term cell exposure scenarios	6
2.1.5 Cytotoxicity measurements	7
2.2 PIXE sample exposures	8
2.2.1 PIXE setup	8
2.2.2 ENM Sample preparation	10
2.2.3 Main results for PIXE analysis	11
2.2.4 Conclusions for the PIXE technique	13
2.3 ICP-OES sample exposures	14
2.3.1 Optimisation of acid digestion protocol for ICP-OES analysis	14
2.3.2 Real concentration under exposure conditions	14
2.3.2 ENM Fate in A549 lung epithelial cells	15
2.3.3 Results for short exposure conditions	15
2.3.4 Results for repeated exposure conditions	17
2.3.5 Results for single, high-dose exposure and 80 h post-incubation	18
2.3.6 Summary of the ICP-OES data	19
2.4 Enhanced hyperspectral imaging	23
2.5 Fate of ENM in a 3D liver model (HWU, InSphero, NRCWE)	24
2.6 Final conclusions	24
<b>3. DEVIATIONS FROM THE WORKPLAN TO BE COMPLETED</b>	<b>26</b>
<b>4. PERFORMANCE OF THE PARTNERS</b>	<b>27</b>
<b>5. CONCLUSIONS</b>	<b>28</b>
<b>6. ANNEX:</b>	<b>29</b>

## 1. Description of task

### TASK 1.4 Fate in *in vitro* models; (AMI, UNamur, NRCWE, USC); M8-30

This task will assess the interaction of the Tier 1 ENM with the lung, gut and liver models from WP3-5. The biological interaction tests will be conducted by AMI. This approach will consider material uptake, intracellular fate and translocation across the cellular membrane within each test system. The analytical tools to detect and quantify the different materials will include spectroscopic and imaging methods, e.g. ICP-OES, ICP-MS, flow cytometry, light and electron microscopy techniques (method selection will be dictated by the material type) (AMI, UNamur, USC). During the first phase the focus will be on epithelial cells from different 3D models provided by WP3 and WP4. Uptake, intracellular fate and translocation will be assessed. For the lung and gut co-culture models, transfer of ENM into the lower medium chamber will provide the measure for translocation. For the 3D liver microtissue model, nanoscale imaging will provide the necessary fate data. Transformations on the ENM's surface and bulk, due to interactions with at least two *in vitro* models, will be evaluated with spectroscopic (XPS) and ion beam analysis techniques, such as, ( $\mu$ )PIXE (UNamur). The delivered dose will be calculated from the ENM's sedimentation considering also data and models tested as part of Task 1.2 as well as compartmental biodissolution and reactivity data generated in Task 1.3 (NRCWE, UNamur). Data relevant to the concentration-dependent impact upon the ENM-cell (system) interaction will then be provided to WP6, Task 6.2 in order to model the predictive delivered concentration of the ENM on the cell surface.

## 2. Description of work & main achievements

**AMI** was responsible for coordinating the different experiments within Task 1.4 such as exposure of ENM Tier1 materials to two different epithelial cell types, *i.e.* the A549 cell line (adenocarcinomic human alveolar basal epithelial type II cells) as well the Caco-2 cell line (human epithelial colorectal adenocarcinoma) used in WP3 and WP4, and the analytics to detect and quantify the different materials in different fractions, *i.e.* apical, basal and cellular, with the partner institutions ISTECE and UNamur.

**UNamur** determined the ENM concentration from samples provided by AMI (apical, basal and cell fractions). UNamur improved an existing setup for the measurement of biological samples (ENM in cell culture medium). First, they started measuring samples that were dried before the analysis. The initial results were not satisfactory; therefore, they invested a lot of effort in improving the existing Particle Induced X-Ray Emission (PIXE) setup. They developed different versions of sample holders and finally designed a holder that contains 6 µL of liquid sample with a rotatory device (to avoid sedimentation issues). The description of the work realised, and the results are described in the following sections.

**ISTEC** added to the study of ENMs interaction with the two different epithelial cells and translocation across the barrier, by applying spectroscopic methods, *i.e.* inductively coupled plasma optical emission spectroscopy (ICP-OES).

**NRCWE** imaged the distribution of ENM in 3D liver microtissues prepared by **HWU** and **InSphero**.

### 2.1 Experimental part

#### 2.1.1 Cell cultures

Both epithelial cell types were grown at AMI on permeable transwell membrane inserts provided by Corning ([www.corning.com](http://www.corning.com)) (**Fig. 1**) (12-well formats were used with 3.0 µm pores) and the initial investigation focused on the preparation of lung and intestinal epithelial monolayers including the evaluation of the cell seeding number and duration of culture stability of each cell line, both under submerged conditions. The cell cultures were characterised regarding monolayer formation (*i.e.* assessed by morphology visualisation), epithelial tissue layer tightness (*i.e.* investigated via immunostaining of actin filaments and trans-epithelial electrical resistance measurement (TEER)). The A549 cells were cultured for 5 days in complete RPMI cell culture medium and the Caco-2 cells were cultured for 21 days in complete DMEM cell culture medium, both under submerged conditions to form a proper monolayer according to the SOPs provided by WP3 and WP4. (**Fig. 2**)



**Figure 1:** Image of transwell membrane insert used. (taken from Corning.com (accessed 24.07.19)).

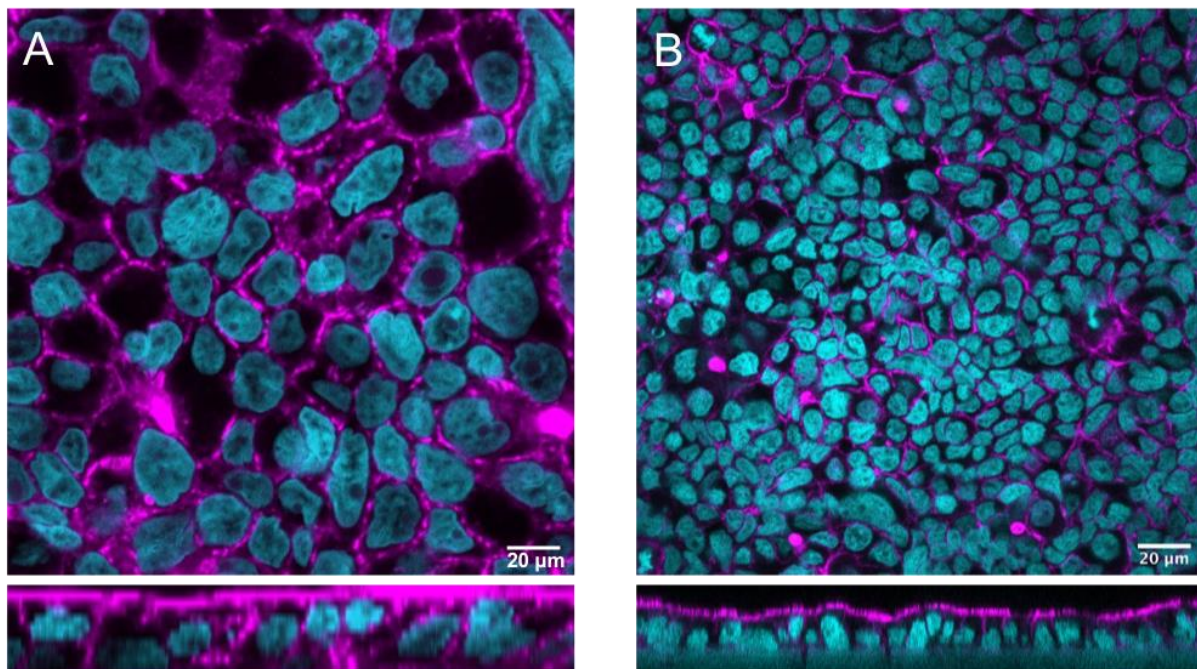


**Figure 2:** Caco-2 (A) and A549 (B) monolayer formation after 21 days and 5 days of cell seeding. F-Actin filaments (magenta), cell nuclei (cyan).

### 2.1.2 ENM Materials (Tier1)

Titanium dioxide ( $\text{TiO}_2$ ), NM-105, and Zinc oxide ( $\text{ZnO}$ ), NM-110 and NM-111, were provided as nano-powders by JRC in Ispra (Italy). Barium sulphate ( $\text{BaSO}_4$ ), NM-220, Cerium dioxide ( $\text{CeO}_2$ ), NM-212 and Silica dioxide ( $\text{SiO}_2$ ), NM-200 were purchased from Fraunhofer-Gesellschaft (Germany). Crystalline silica, DQ12, was provided by Robock. The dissolved ionic Ba, Ce, Si, Ti and Zn standard for ICP-OES, hydrogen peroxide solution (95321) and nitric acid (84380-M) were purchased from Sigma-Aldrich (St. Louis, MO, US).

### 2.1.3 ENM Sample preparation

Samples were prepared starting from stocks at  $2.56 \text{ mg mL}^{-1}$  in MilliQ water + BSA, prepared accordingly to the NANoREG dispersion protocol. The stocks were then diluted in DMEM or RPMI +10 % FBS medium reaching the desired concentration in the concentration range of  $12.5 - 100 \mu\text{g/mL}$ .

### 2.1.4 Short- and long-term cell exposure scenarios

For the first studies to optimise the analytical methods, we exposed A549 and Caco-2 cells at 10 and  $100 \mu\text{g/mL}$  of ENMs for 24 h. In the long-term repeated exposures on A549 cells, two scenarios were evaluated under submerged conditions. In the first scenario, the cells were exposed repeatedly every day up to 5 days, using  $25 \mu\text{g/mL}$  ENMs concentration, resulting in a total exposure of  $100 \mu\text{g/mL}$  and 5 days incubation time in total. Apical, wash and basal samples were collected after 24 h, 48 h, 72 h and 80 h of exposure, while the cell fraction was collected at the end of the experiment at 80 h (see Figure 3). In the second scenario, cells were exposed to a single  $100 \mu\text{g/mL}$  dose of ENMs at day 0 for 5 days.

To analyse the cellular uptake of the material, whole membranes with the cells attached were cut out. All measurements were done in triplicates and three repetitions ( $n = 3$ ). Sampling was performed at AMI, whilst PIXE measurements were performed at UNamur and ICP-OES measurements were performed at ISTE, following the optimised procedure as described below.

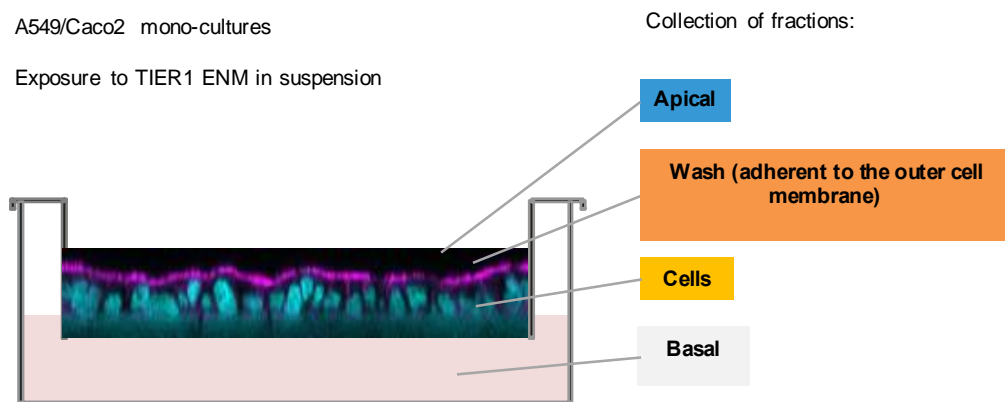


**Figure 3:** Schematic indicating the sample collection after ENM exposure to A549 or Caco-2 cell cultures.

### 2.1.5 Cytotoxicity measurements

Due to long-term repeated exposures, cytotoxicity of the A549 cells exposed to 100  $\mu\text{g}/\text{mL}$  of ZnO, BaSO<sub>4</sub>, CeO<sub>2</sub>, DQ12 and TiO<sub>2</sub> for 80 h was assessed via quantification of LDH released into the apical and basal cell culture medium. No significant cytotoxicity was observed after 80 h following exposure compared to untreated cells, whereas a significant increase could be shown for the positive control (Triton-X-100).

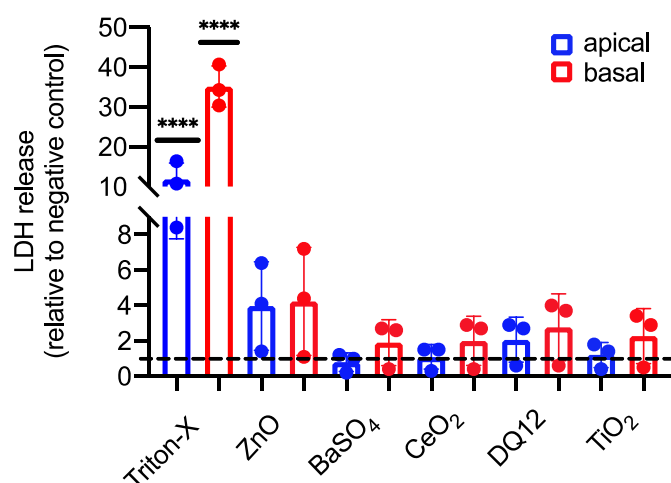


**Figure 4:** Cytotoxicity determined by measuring the release of lactate dehydrogenase (LDH) by A549 cells after the exposure of 100  $\mu\text{g}/\text{mL}$  ZnO, BaSO<sub>4</sub>, CeO<sub>2</sub>, DQ12 and TiO<sub>2</sub> for 80 h. A total of three independent experiments ( $n = 3$ ), consisting of three single replicates each, were performed. Statistically significant difference to the positive control is denoted by asterisks, where \*\*\* is  $p < 0.0001$ .

## 2.2 PIXE sample exposures

Initial studies conducted to elaborate a suitable protocol for **PIXE** quantification included, several series using  $\text{TiO}_2$  nanoparticles (NPs) dispersed in ultrapure water for calibration purposes and material testing of  $\text{BaSO}_4$  (NM-220) and  $\text{CeO}_2$  (NM-212) at concentrations of 1, 10 and 100  $\mu\text{g/mL}$  for 24 h.

### 2.2.1 PIXE setup

Ion Beam Analysis (IBA) techniques such as Particle-Induced X-ray Emission (PIXE) are well suited to quantify the concentration of ENMs in complex matrices, e.g. complete cell culture medium. Usually, PIXE measurements are simultaneously performed with Elastic Backscattering Spectrometry (EBS). In this case, the EBS spectra are used to derive the number of incident particles hitting the sample under analysis (*i.e.* the so-called incident charge), which is used in turn to quantify the NPs concentration (down to a few wt.ppm) from the PIXE spectra.

This is a very powerful technique broadly used in various research fields, but this EBS-PIXE combination generally requires the sample to go under vacuum, which becomes a serious issue when intending to measure liquid samples. In this case, two options are available: (i) the liquid sample is freeze-dried, and the dried matter is placed on a substrate to go under vacuum, or (ii) a special cell is designed with an ultrathin entrance window through which the ion beam analysis is performed.

After a series of tests, the first option has unfortunately been proved to be unusable. Indeed, we have demonstrated that the topography of the dried matter obtained by freeze-drying the liquid sample was close to the illustration shown in Figure 5. The non-uniformity of the thickness of dried matter deposited on the substrate is highly problematic for the data processing because of the self-absorption of X-rays in the sample. Besides, since the spot size of the incident ion beam is smaller than the area on which the dried matter is deposited, « we are unable to quantify the amount of dried matter during the analysis (expressed in  $\mu\text{g}/\text{cm}^2$ ) and therefore no means of quantifying the EMN's concentration.

This has been experimentally demonstrated by introducing a very thin gold (Au) layer (*i.e.* ~10 nm; deposited by Physical Vapour Deposition process; Au is not expected to be present in the liquid samples) on the carbon substrate before freeze-drying the liquid sample. The large variability of the Au signal observed by PIXE by moving the incident ion beam across one sample or from one sample to another, proves the significant non-uniformity of the dried matter obtained by a freeze-drying process.

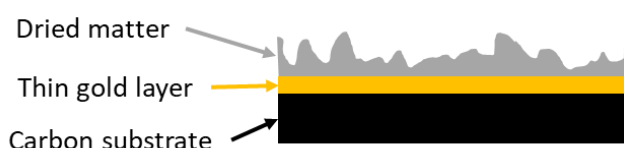


**Figure 5:** Illustration of a sample obtained by freeze-drying liquid on a thin gold layer deposited on a carbon substrate.

The setup that is described next is the final one. Indeed, we have undertaken several steps of improvement in the design of the sample holder and the system of detection (detectors and configuration). We have gone from the preparation of dried samples to the direct analysis of liquid samples, in between we designed different sample holders for different volumes optimising the conditions of the analysis. During the analysis of different series of samples, we have learned some specificities in the sample preparation. For example, some ENMs seems to sediment faster in the culture medium, such as TiO<sub>2</sub>. This requires some specific handling before the analysis, especially for the preparation of controls made of ENMs in water only.

Most of the modifications in the sample holder were guided by the comprehension of the evaporation phenomenon of samples, going from liquid to solid-state. After evaluation, the liquid samples were chosen over the dried ones. However, due to limitations of the technique reaching the Limit Of Detection (LOD), we had to concentrate samples to obtain values with acceptable uncertainty values. The concentration-time, with an air pulsed oven, was ENMs dependant. The system of detection is illustrated in the following Figure 6.

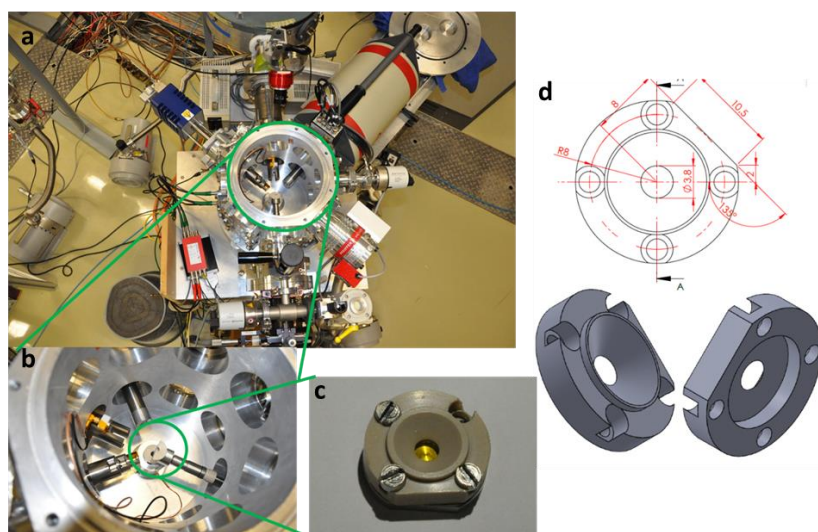


**Figure 6:** Setup for PIXE analysis of liquid samples. a) Chamber of analysis (top view), b) Three detectors (left side) and the sample holder (right side), c) Sample container and d) details and cross-view of the sample container.

The final design is the development of a “liquid cell” that directly brings the liquid under vacuum to perform the analysis. Schematics of this liquid cell is shown below (Figure 7). A small volume of the liquid sample (i.e.  $\pi \cdot 2^2 \cdot 0.5 = 6 \mu\text{l}$ ) is placed on a stainless steel (SS) substrate and sealed with a 12- $\mu\text{m}$  thick foil of Mylar or Kapton. This foil is thick enough to withstand a pressure of 1 atm over this area, therefore confining the liquid under these vacuum conditions.

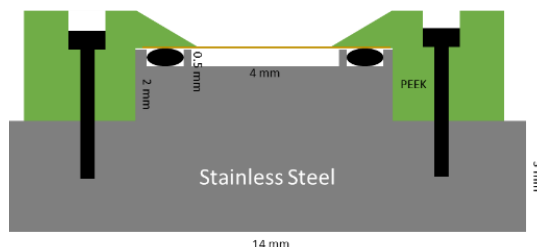


**Figure 7:** “Liquid cell” developed at UNamur to enable the analysis of liquid under vacuum by EBS-PIXE.

This “liquid cell” is then placed under vacuum ensuring than no metallic part is visible for the incident beam. This precaution is to monitor the quality of the sealing during the measurement. Indeed, the projected range of 2.5 MeV proton beam into water is about 110 µm. With a good “liquid cell” sealing, the incident beam is stopped within the liquid and does not reach the SS substrate. However, if the sealing fails, the liquid will slowly evaporate under vacuum leading to thinning of the liquid layer, and the Fe-Cr-Ni signals typical of SS will come up in the PIXE spectrum. Finally, we have developed a sample holder allowing us to rotate the “liquid cell” during the measurement to minimise the sedimentation of ENMs during the analysis. Each analysis last between 5 and 10 min.

In terms of detection setup, we have duplicated the particle detectors (EBS-detectors) as well as the X-rays detectors (PIXE-detectors). This allows us to have internal checks for the determination of the incident charge (i.e. number of incident particles) as well as for the PIXE quantitation: each detector being handled independently from each other, the 2 EBS-detectors and the 2 PIXE-detectors must agree with each other. Besides, for the PIXE detectors, we have used an Ultra-LEGe with a thick (250 µm) Mylar filter to get more sensitivity to high energy (i.e. > 15 keV) X-rays, combined with an SDD (Silicon Drift Detector) used with a magnetic filter to get more sensitivity to low energy (i.e. < 10 keV) X-rays.

It should be noted that the very small volume required for the analysis (~6 µL) allows the concentration (by evaporation) of the liquid samples to be determined. This improves the limit of detection down to a few wt.ppm. The protocol to concentrate the samples must nevertheless be improved and probably adapted to each kind of ENMs under interest. Each type of ENMs, having specific physicochemical characteristics, therefore requires modifications in the sample preparation.

### 2.2.2 ENM Sample preparation

Several series using TiO<sub>2</sub> ENMs dispersed in ultrapure water were prepared for calibration purposes. One main problem was observed: the sedimentation of the ENMs after preparation of the dispersion, right before the analysis and during the actual analysis. To remediate this, we conducted all the measurements with a rotatory device to avoid the sedimentation as much as possible. Results show that the PIXE technique can produce reliable data as illustrated by the calibration curve in Figure 8.

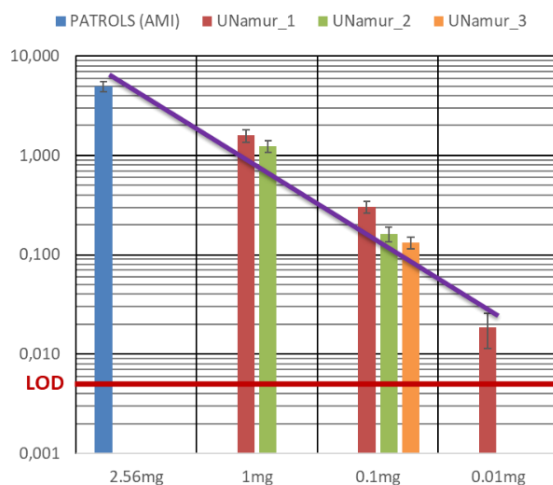


**Figure 8:** Calibration curve with  $\text{TiO}_2$  dispersed in ultrapure water measured with PIXE technique (LOD: Limit of Detection).

### 2.2.3 Main results for PIXE analysis

$\text{BaSO}_4$  (NM-220),  $\text{SiO}_2$  (NM-200), DQ12,  $\text{TiO}_2$  (NM-105),  $\text{ZnO}$  (NM-110) and  $\text{CeO}_2$  (NM-212), with a nominal concentration of 100  $\mu\text{g/mL}$  for 24 h (Figure 9) were exposed to A549 and Caco-2 cells. Samples with lower concentrations were not considered. Several experiments were performed in order to reach the final setup required for analysis of the samples with the PIXE technique. For example, the analysis of  $\text{CeO}_2$  (NM-212) and  $\text{BaSO}_4$  (NM-220) were previously successfully achieved. However, the experimental conditions were slightly different. For this reason, these data are not present here. In the previous analysis, we conclude that samples with a lower concentration than 0.01 mg/mL produced high uncertainty values. The concentration of 0.001 mg/mL is below the LOD of this technique. For this reason, and given that the LOD was similar to the expected values, we decided not to continue with the analysis of these samples.

We were not able to establish a protocol for the measurement of samples containing the cells (grown on top of the insert membrane), due to the difficulty in evaluating their total mass- a required to calculate the concentrations by the PIXE methodology. In the case of the “wash samples”, the concentration determined was lower than the LOD or the measurements were not reproducible. Therefore, these measurements are not reported.

Figure 9 and Table 1 illustrate the last series of results for the experiment with A549 cells measured at the same conditions (liquid sample, rotation system, same protocol for sample preparation).

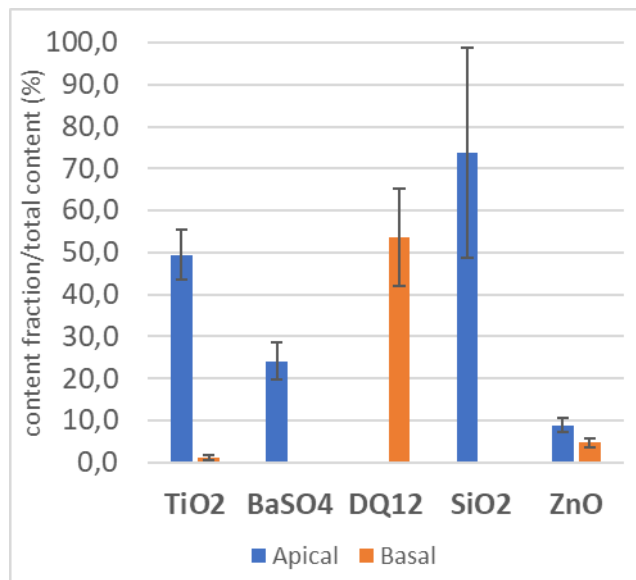


**Figure 9:** Single short term exposure of TiO<sub>2</sub> NM-105, BaSO<sub>4</sub> NM-220, DQ12, SiO<sub>2</sub> NM-200 and ZnO NM-110 at concentrations of 100 µg/ml for 24 h to A549 cells obtained by PIXE. (n = 3)

	TiO <sub>2</sub> NM-105	BaSO <sub>4</sub> NM-220	DQ12	SiO <sub>2</sub> NM-200	ZnO NM-110
<b>Apical</b>	49,5	24,2	0,0	73,9	8,9
<b>Basal</b>	1,1	0,0	53,6	0,0	4,7
<b>Uncertainty A</b>	5,9	4,3	0,0	25,0	1,7
<b>Uncertainty B</b>	0,6	0,0	11,6	0,0	1,1

**Table 1:** Concentrations of the apical and basal fractions in A549 cells in µg/mL, measured by PIXE.

Figure 10 and Table 2 illustrate the last series of results measured under the same conditions for the experiments with Caco-2 cells.

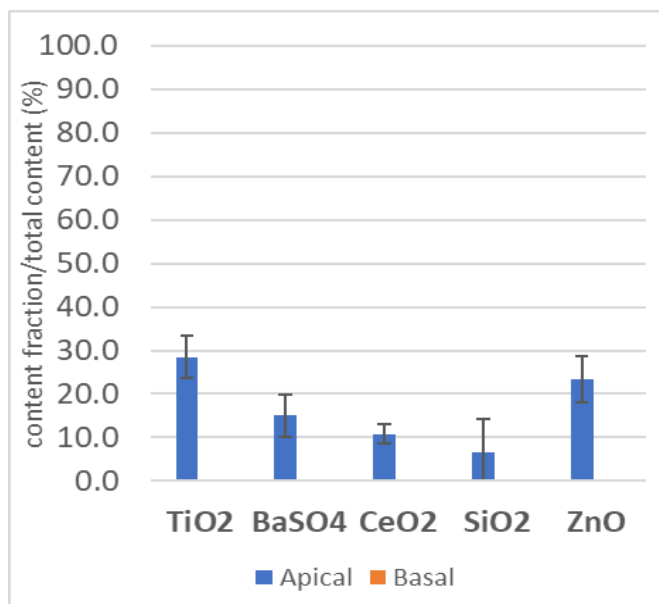


**Figure 10:** Single short term exposure of TiO<sub>2</sub> NM-105, BaSO<sub>4</sub> NM-220, CeO<sub>2</sub> NM-212, SiO<sub>2</sub> NM-200 and ZnO NM-110 at concentrations of 100 µg/mL for 24 h to Caco-2 cells obtained by PIXE. (n = 3)

	TiO <sub>2</sub> NM-105	BaSO <sub>4</sub> NM-220	CeO <sub>2</sub> NM-212	SiO <sub>2</sub> NM-200	ZnO NM-110
<b>Apical</b>	28.4	15.0	10.8	6.7	23.4
<b>Basal</b>	0.0	0.0	0.0	0.0	0.0
<b>Uncertainty A</b>	4.9	4.8	2.2	7.5	5.2
<b>Uncertainty B</b>	0.0	0.0	0.0	0.0	0.0

**Table 2:** Concentrations of the apical and basal fractions in Caco-2 cells in µg/mL, measured by PIXE.

#### 2.2.4 Conclusions for the PIXE technique

The results obtained by the PIXE technique show values measured for the apical and basal fractions (percentage with respect to nominal dose). Apical fraction values go from higher to lower for the SiO<sub>2</sub> NM-200, TiO<sub>2</sub> NM-105, BaSO<sub>4</sub> NM-220 and ZnO NM-110 respectively. This tendency is similar to the results obtained by ICP-OES (see next sections), except for the SiO<sub>2</sub> NM-200. No valuable information for the CeO<sub>2</sub> NM-212 was obtained, for either fraction (concentrations below the LOD). For the DQ12, only the basal fraction was measured. The PIXE technique was not able to produce data for all the conditions. In some cases the LOD was too high, despite the concentration step (evaporation in an oven) of the liquid samples. In the case of the experiment with Caco-2 cells, only values for the apical fraction were obtained. These results suggest that most of the ENMs are retained in the cells and cellular membranes. The values obtained are comparable for both experiments, A549 and Caco-2 cells, with exception of the SiO<sub>2</sub> NM-200. Some improvements in the settings are still possible to lower the LOD, however, the timing required for this, and the Covid-19 situation, restricted this possibility. The same happened with the µPIXE measurements that were not finally performed. The impact of Covid-19, and

lockdown on the development of these settings and on the calibration of the system should not be underestimated.

### 2.3 ICP-OES sample exposures

#### 2.3.1 Optimisation of acid digestion protocol for ICP-OES analysis

The real concentration of ENMs in selected media was evaluated by inductively coupled plasma optical emission spectrometry (ICP-OES) using an ICP-OES 5100 – vertical dual view apparatus coupled with OneNeb nebuliser (Agilent Technologies, Santa Clara, CA, USA). A digestive procedure was performed by adding 0.2 mL of hydrogen peroxide ( $\text{H}_2\text{O}_2$  30 wt% in water) and 0.2 mL of nitric acid ( $\text{HNO}_3$  65 %) into 0.5 mL sample and filling with 1.5 mL of MilliQ water. The treated samples were ultrasonicated for 10 min in an ultrasonic bath (Bath Temperature = 50°C) and then analysed by ICP-OES. Calibration curves were obtained with 0.01, 0.05, 0.1, 1.0, 10.0 and 50.0  $\mu\text{g mL}^{-1}$  standards, sample's medium (RPMI or DMEM+10 % FBS) was used as a matrix, and the same digestive procedure was applied to standards. For wavelength, we selected Ba 233.5 nm, Ce 418.7 nm, Si 251.6 nm, Ti 334.9 nm and Zn 206.2 nm.

The optimisation of the acid digestion protocol allowed detection of the real concentration of ENMs in relevant media, including DMEM or RPMI containing 10 % FBS, checking any deviations from the nominal one. Three stocks at 12.5, 50 and 100  $\mu\text{g mL}^{-1}$  in DMEM + 10 % FBS were prepared by adding powder (avoiding the use of probe sonicator) and acid digested. Three different acid digestive receipts were evaluated, using only nitric acid, nitric acid and hydrogen peroxide or the mix of nitric, sulfuric and phosphoric acids. The acid digestion based on the use of nitric acid and hydrogen peroxide, coupled with OneNeb nebuliser, was identified as the better procedure, because it limited interference of sulfuric and phosphoric acids in spectroscopy elemental detection and resulted in all samples achieving a recovery of above 95 %. Once the best acid digestive receipt was selected, we applied it to determine the real ENM concentration of working suspensions obtained by thawing frozen stocks, prepared following the NANoREG dispersion protocol, and diluting them in biological media (DMEM + 10 % FBS and RPMI + 10 % FBS) at 10 and 100  $\mu\text{g mL}^{-1}$ . Each sample was prepared in triplicate and analysed by ICP-OES.

#### 2.3.2 Real concentration under exposure conditions

The real concentrations of working suspensions are reported in Tables 3 and 4. The measured concentrations were always lower than the nominal ones, in both media, due to partial loss of material during the operational steps (dispersion and dilution). Therefore, the check of nominal concentration is always recommended on the stocks, before their use in cell culture tests.

NPs	Nominal conc. expected ( $\mu\text{g mL}^{-1}$ )	Measured conc. ( $\mu\text{g mL}^{-1}$ )	STD dev ( $\mu\text{g mL}^{-1}$ )	% Detected
Ag sigma	100	63.57	0.19	64
	10	6.50	0.38	65
SiO <sub>2</sub> IUF	100	39.36	4.83	39
	10	4.19	0.20	42
BaSO <sub>4</sub>	100	56.50	8.39	56
	10	5.67	0.23	57
CeO <sub>2</sub>	100	67.48	14.19	67
	10	6.38	1.15	64

**Table 3:** ENMs concentration in DMEM + 10 % FBS medium, expressed as percentage of real NPs concentration over nominal one.

NPs	Nominal conc. expected ( $\mu\text{g mL}^{-1}$ )	Measured conc. ( $\mu\text{g mL}^{-1}$ )	STD dev ( $\mu\text{g mL}^{-1}$ )	% Detected
TiO <sub>2</sub> 105	100	77.56	3.44	78
	10	5.42	0.46	54
DQ12	100	51.74	1.33	52
	10	5.65	0.29	56
BaSO <sub>4</sub>	100	63.20	1.58	63
	10	6.55	0.45	65
CeO <sub>2</sub>	100	35.21	3.45	65
	10	5.27	0.64	53
ZnO 110	100	82.9	3.72	83
	10	9.07	0.52	91
ZnO 111	100	90.60	3.73	91
	10	8.91	0.52	89

**Table 4:** ENMs concentration in RPMI + 10 % FBS medium, expressed as percentage of real ENMs concentration over nominal one.

### 2.3.2 ENM Fate in A549 lung epithelial cells

For the ICP-OES studies done at ISTE, only experiments with A549 cells could be performed by AMI as the optimisation of the material analysis took longer than planned.

### 2.3.3 Results for short exposure conditions

Single exposure measurements were performed for all ENMs ( $\text{BaSO}_4$  NM-220,  $\text{CeO}_2$  NM-212, DQ12,  $\text{TiO}_2$  NM-105 and  $\text{ZnO}$  NM-111) using  $100 \mu\text{g mL}^{-1}$  for 24 h. After 24 h of exposure,  $\text{ZnO}$  NM-111,  $\text{BaSO}_4$  NM-220,  $\text{CeO}_2$  NM-212 and  $\text{TiO}_2$  NM-105 showed only few translocations of the materials across the cell monolayer into the basal compartment. Most amounts of the materials were found in the apical, as well as the wash fraction, see Table 5 and Figure 11. A different outcome was observed for DQ12, where most of the material could be found in the cell fraction, whereas a lower but equal amount was found in the apical and basal fraction.

Compartment	$\text{BaSO}_4$ NM-220	$\text{CeO}_2$ NM-212	DQ12	$\text{TiO}_2$ NM-105	$\text{ZnO}$ NM-111
	[ $\mu\text{g mL}^{-1}$ ]				
Apical	$19.75 \pm 4.54$	$16.02 \pm 2.22$	$2.56 \pm 0.77$	$57.41 \pm 11.40$	$20.58 \pm 1.31$
Wash	$3.69 \pm 2.31$	$3.65 \pm 1.76$	$3.01 \pm 1.66$	$1.45 \pm 0.18$	$5.31 \pm 2.55$
Basal	$0.99 \pm 0.50$	$0.70 \pm 0.59$	$0.50 \pm 0.20$	$1.09 \pm 1.06$	$6.95 \pm 1.25$
Cells	$10.64 \pm 3.10$	$3.04 \pm 1.24$	$9.02 \pm 3.89$	$1.31 \pm 0.25$	$1.50 \pm 0.21$
Stock 100 ( $\mu\text{g mL}^{-1}$ )	$57.71 \pm 5.44$	$39.83 \pm 6.64$	$62.19 \pm 42.09$	$104.04 \pm 14.34$	$63.52 \pm 0.76$
Stock stock 2000 ( $\mu\text{g mL}^{-1}$ )	$759.24 \pm 479.37$	$949.35 \pm 6.43$	$1685.69 \pm 3.71$	$1649.57 \pm 24.77$	$1382.51 \pm 12.47$

**Table 5: Short exposure conditions.** Nominal concentration of  $\text{BaSO}_4$  NM-220,  $\text{CeO}_2$  NM-212, DQ12,  $\text{TiO}_2$  NM-105 and  $\text{ZnO}$  NM-111 in all fractions exposed to  $100 \mu\text{g mL}^{-1}$  after 24h. A total of three independent experiments ( $n=3$ ), consisting of three single replicates each, were performed. All data are presented as mean  $\pm$  standard deviation.

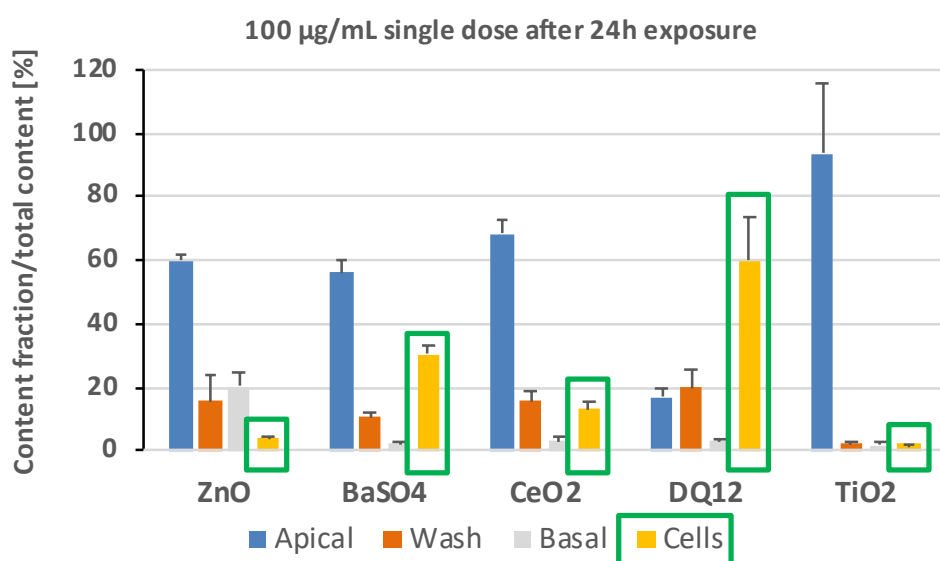


**Figure 11:** Single short term exposure of ZnO NM-111, BaSO<sub>4</sub> NM-220, CeO<sub>2</sub> NM-212, DQ12 and TiO<sub>2</sub> NM-105 at concentrations of 100 µg/mL for 24 h to A549 cells. A total of three independent experiments ( $n=3$ ), consisting of three single replicates each, were performed.

### 2.3.4 Results for repeated exposure conditions

Repeated exposure measurements were performed for all ENMs (BaSO<sub>4</sub> NM-220, CeO<sub>2</sub> NM-212, DQ12, TiO<sub>2</sub> NM-105 and ZnO NM-111) exposing the cells to 25 µg/mL at days 0, 1, 2, 3, and 4 and sample collection was performed at 24, 48, 72 and 80 h (Figure 12 and Table 6). The cell fractions were collected only after the 80 h time point. For BaSO<sub>4</sub> NM-220, the majority of the material could be detected in the apical fraction, and after 80 h of exposure, a small amount of ENMs was found inside the cells, and only a low concentration was detected in the basal fraction. Similar behaviour was observed for CeO<sub>2</sub> NM-212. For TiO<sub>2</sub> NM-105, we could not detect any material translocation and limited cellular uptake, the majority of the mass was in the apical fraction. A low concentration was found in the wash and cells compartment with no penetration into the basal one, indeed, sometime in the daily exposure the concentration values in the basal section were lower than the ICP-OES limit of detection (< 0.01 µg mL<sup>-1</sup>). For ZnO NM-111 samples, we detected similar concentrations in the apical and basal compartments after the first 24h, and this trend continued up to 5 days. A low concentration of ZnO NM-111 was detected in the wash and cell samples. A different distribution pattern was observed for DQ12. After the first 24h, DQ12 was mainly detected in the apical compartment, and lower concentrations were also detected in the basal and wash samples. After 5 days, a clear decrease in the apical fraction could be observed while the concentrations in the basal compartment stayed constant. After 80 h of exposure, a significant concentration of DQ12 was detectable in the cell fraction.

Samples daily exposed to 25 µg mL <sup>-1</sup>	Exposure time (h)	BaSO <sub>4</sub> (µg mL <sup>-1</sup> )	CeO <sub>2</sub> (µg mL <sup>-1</sup> )	DQ12 (µg mL <sup>-1</sup> )	TiO <sub>2</sub> (µg mL <sup>-1</sup> )	ZnO (µg mL <sup>-1</sup> )
Apical	24	9.49 ± 1.54	5.96 ± 1.51	8.89 ± 1.57	17.31 ± 1.71	14.45 ± 3.02
Wash		0.84 ± 0.74	0.40 ± 0.12	1.02 ± 1.20	0.04 ± 0.05	0.08 ± 0.08
Basal		0.20 ± 0.00	0.03 ± 0.04	2.13 ± 1.28	0.00 ± 0.00	7.88 ± 0.87
Apical	48	8.89 ± 1.05	4.89 ± 1.02	9.08 ± 0.37	15.62 ± 0.56	13.41 ± 0.76
Wash		0.32 ± 0.03	0.26 ± 0.10	5.90 ± 2.42	0.06 ± 0.04	0.04 ± 0.03
Basal		0.64 ± 0.31	0.04 ± 0.05	1.30 ± 5.04	0.00 ± 0.00	7.85 ± 0.41
Apical	72	8.30 ± 0.37	3.96 ± 0.84	6.61 ± 1.40	9.42 ± 2.69	12.12 ± 1.28
Wash		0.27 ± 0.00	0.48 ± 0.07	7.26 ± 2.19	0.00 ± 0.00	0.04 ± 0.05
Basal		0.27 ± 0.02	0.04 ± 0.04	2.36 ± 0.55	0.00 ± 0.00	8.09 ± 0.42
Apical	80	10.12 ± 1.15	4.40 ± 0.99	6.90 ± 1.47	7.91 ± 0.88	16.57 ± 0.68
Wash		0.34 ± 0.06	0.46 ± 0.09	5.58 ± 2.08	0.00 ± 0.00	0.17 ± 0.09
Basal		0.18 ± 0.03	0.07 ± 0.06	4.03 ± 1.41	0.09 ± 0.03	3.39 ± 0.34
Cells	80	0.91 ± 0.24	0.29 ± 0.04	5.55 ± 1.04	0.04 ± 0.04	0.01 ± 0.03
STOCK 25 (µg mL <sup>-1</sup> )	-	9.60 ± 0.23	10.46 ± 0.14	9.27 ± 0.47	15.16 ± 0.24	22.26 ± 0.97

**Table 6:** Long repeated exposures. Nominal concentration of BaSO<sub>4</sub> NM-220, CeO<sub>2</sub> NM-212, DQ12, TiO<sub>2</sub> NM-105 and ZnO NM-111 in all compartments for daily exposure to 25 µg mL<sup>-1</sup>. A total of three independent experiments ( $n=3$ ), consisting of three single replicates each, were performed. All data are presented as mean ± standard deviation.

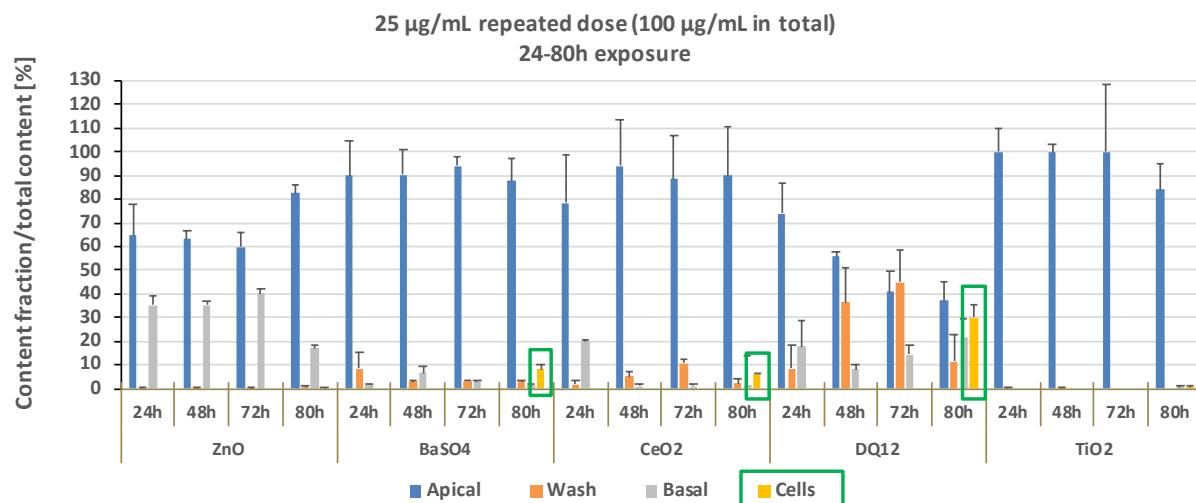


**Figure 12:** Repeated long term exposure of ZnO NM-111, BaSO<sub>4</sub> NM-220, CeO<sub>2</sub> NM-212, DQ12 and TiO<sub>2</sub> NM-105 at concentrations of 25 µg/mL for 24, 48, 72 and 80 h to A549 cells. A total of three independent experiments ( $n=3$ ), consisting of three single replicates each, were performed.

### 2.3.5 Results for single, high-dose exposure and 80 h post-incubation

Exposure measurements were performed for all ENMs (BaSO<sub>4</sub> NM-220, CeO<sub>2</sub> NM-212, DQ12, TiO<sub>2</sub> NM-105 and ZnO NM-111) in A549 cells using one high exposure to 100 µg mL<sup>-1</sup> at day 0 and sample collection was performed after 80 h. Results are reported in Table 7 and Figure 13. BaSO<sub>4</sub> NM-220 is mainly found in the apical section, only low concentrations were detected in the other compartments. After 80 h post-exposure, BaSO<sub>4</sub> NM-220, CeO<sub>2</sub> NM-212 and TiO<sub>2</sub> NM-105 showed low translocation of the materials across the cell monolayer into the basal compartment while for ZnO NM-111 almost the same concentrations could be detected in the apical as well as basal fraction. For DQ12, the majority of the material was found in the apical and cell fraction. All the trends observed for this exposure scenario reflected a similar trend as reported for the repeated exposure scenario.

Samples exposed to 100 µg mL <sup>-1</sup>	Exposure time (h)	BaSO <sub>4</sub> (µg mL <sup>-1</sup> )	CeO <sub>2</sub> (µg mL <sup>-1</sup> )	DQ12 (µg mL <sup>-1</sup> )	TiO <sub>2</sub> (µg mL <sup>-1</sup> )	ZnO (µg mL <sup>-1</sup> )
Apical	80	38.72 ± 1.12	46 ± 14.43	2,60 ± 0,13	48.33 ± 6.52	28,49 ± 2,25
Wash		1.08 ± 0.14	2.39 ± 0.64	0,65 ± 0,18	0.73 ± 0.08	1,30 ± 0,50
Basal		0.87 ± 0.03	0.16 ± 0.17	0,88 ± 0,30	0.00 ± 0.00	23,26 ± 1,53
Cells		1.90 ± 0.15	1.52 ± 0.38	1,48 ± 0,41	0.19 ± 0.18	1,24 ± 0,29

**Table 7:** Nominal concentration of, BaSO<sub>4</sub> NM-220, CeO<sub>2</sub> NM-212 DQ12, TiO<sub>2</sub> NM-105 and ZnO NM-111 in all compartments for single exposure to 100 µg mL<sup>-1</sup> after 80 h.

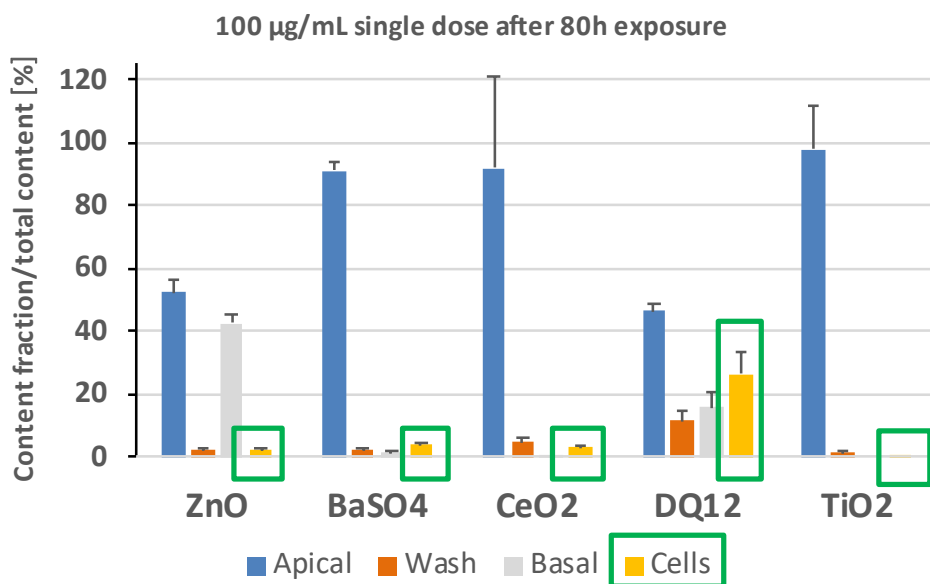


**Figure 13:** Single long term exposure of ZnO NM-111, BaSO<sub>4</sub> NM-220, CeO<sub>2</sub> NM-212, DQ12 and TiO<sub>2</sub> NM-105 at concentrations of 100 µg/mL for 80 h to A549 cells. A total of three independent experiments ( $n=3$ ), consisting of three single replicates each, were performed.

### 2.3.6 Summary of the ICP-OES data

Finally, we summarised the ICP-OES data to evaluate the ENM concentrations in the different fractions for the three exposure scenarios. First, we compared the amounts of ENMs in A549 cells upon exposure to 100 µg/mL ENM after 24 h and 80 h post-exposure (Fig. 14). Interestingly, the ENM content in the cellular fraction decreased from 24 h to 80 h for all materials we investigated. As there was almost no significant change in the other fractions, we assume that the decrease in ENMs content could be associated with multifactorial behaviour. Cells in the epithelial layer could divide resulting in some cell loss, thus diluting the cellular fraction; or they could exocytose NMs, as DQ12 content in the apical and basal fractions increases with time; alternatively, the cells may excrete dissolved ions, as NMs could be solubilised in lysosome. For both ZnO NM-111 and DQ12 an increase in basal concentrations was detected, this could be explained by the solubility of the materials. This is in contrast to the comparison we show in Figure 15. Here, the cells were exposed to a single dose for 24 h and repeatedly to 25 µg/mL over 80 h and an increase of the ENM content in the cellular fraction could be observed for all materials used. Finally, we compare one high concentration exposure at day 0 and repeated exposures over 80 h resulting in the same applied concentrations and analysis of the fractions after 80 h (Fig 16). As demonstrated, the cellular fractions showed a similar content, independent of the exposure.

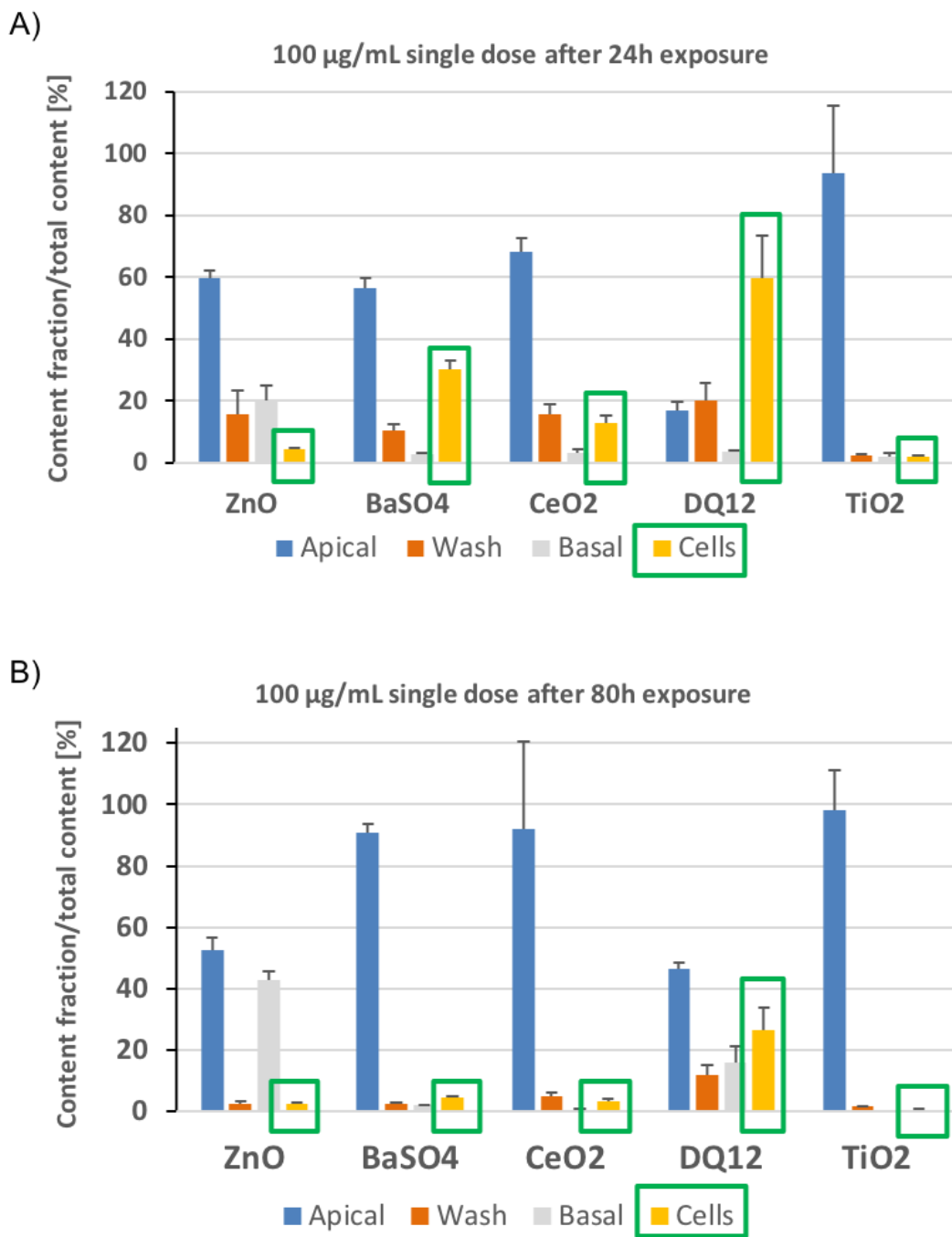


**Figure 14:** Single short term exposure of ZnO NM-111, BaSO<sub>4</sub> NM-220, CeO<sub>2</sub> NM-212, DQ12 and TiO<sub>2</sub> NM-105 at concentrations of 100 µg/ml for 24 h (A) and 80 h (B) to A549 cells. A total of three independent experiments ( $n=3$ ), consisting of three single replicates each, were performed.

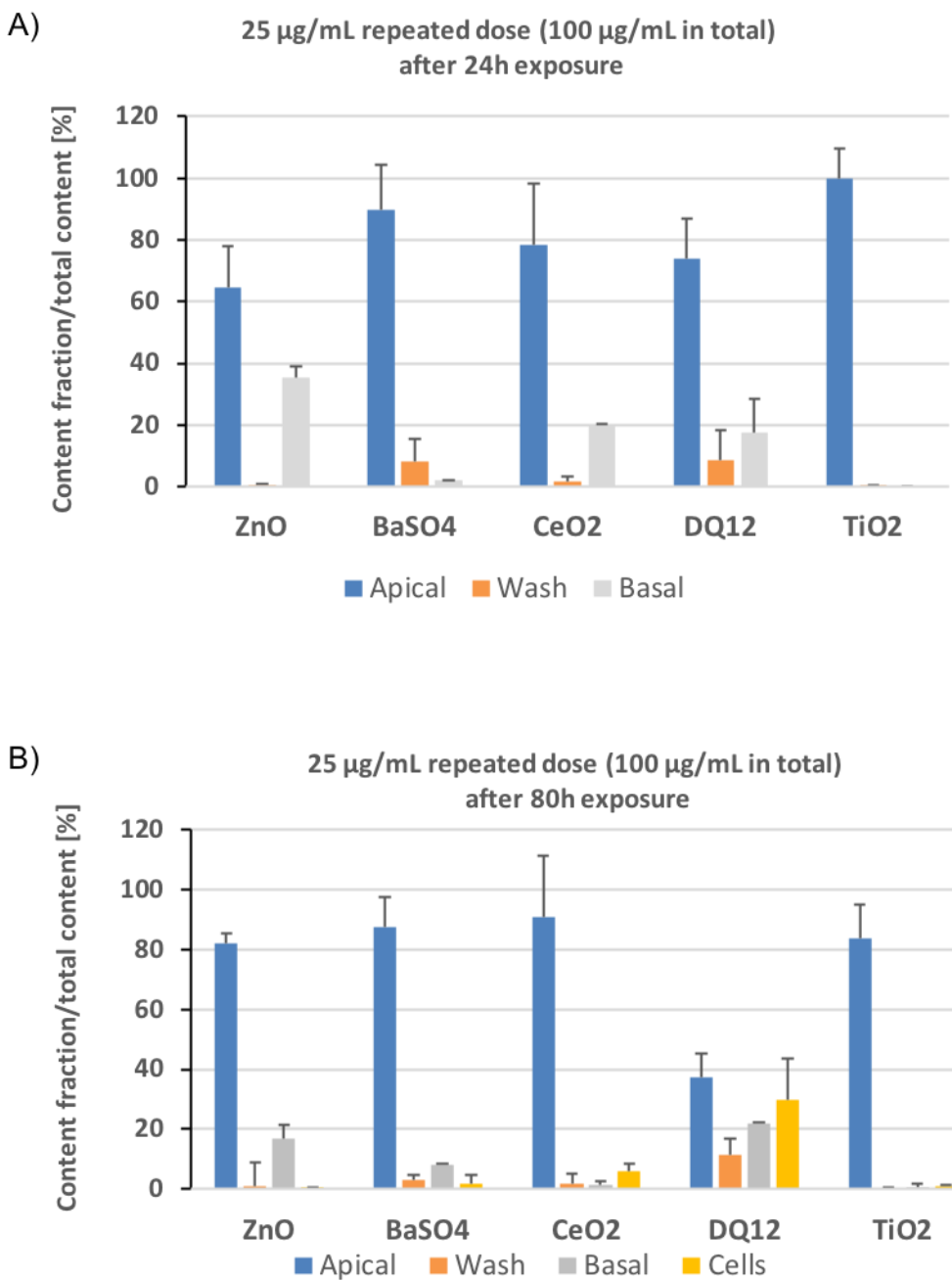


**Figure 15:** Single short term exposure of ZnO NM-111, BaSO<sub>4</sub> NM-220, CeO<sub>2</sub> NM-212, DQ12 and TiO<sub>2</sub> NM-105 at concentrations of 100 µg/mL for 24 h (A) and 80 h (B) to A549 cells and repeated long term exposure with 25 µg/mL over 80 h. A total of three independent experiments ( $n=3$ ), consisting of three single replicates each, were performed.

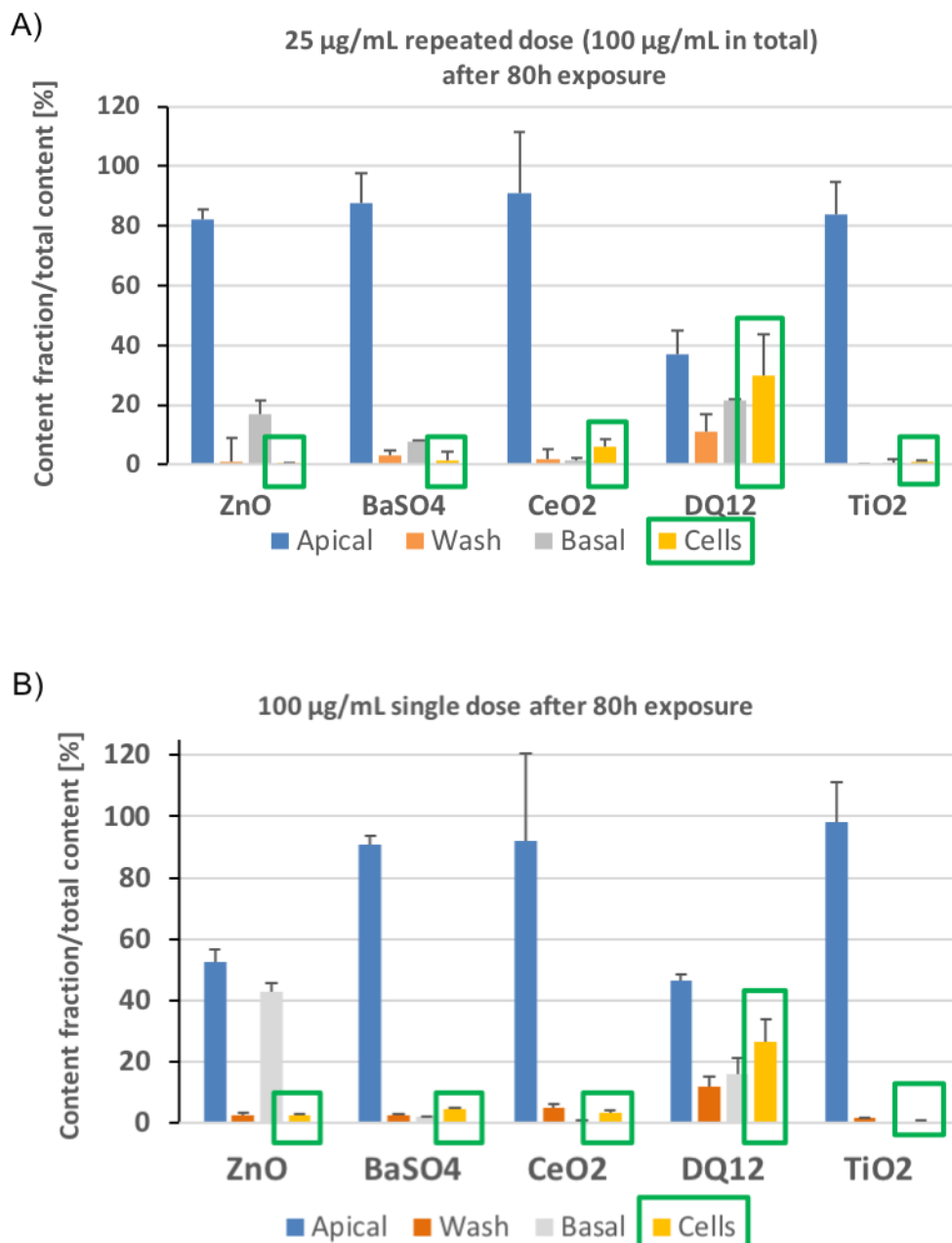


**Figure 16:** Long-term exposure of 25 µg/mL and single exposure of 100 µg/mL of ZnO NM-111, BaSO<sub>4</sub> NM-220, CeO<sub>2</sub> NM-212, DQ12 and TiO<sub>2</sub> NM-105 after 80 h to A549 cells. A total of three independent experiments ( $n=3$ ), consisting of three single replicates each, were performed.

## 2.4 Enhanced hyperspectral imaging

Enhanced hyperspectral imaging (HSI) was performed that allows imaging of cells and particles as well as the spectral confirmation of ENMs. Images with the corresponding spectra are depicted in Figures 17 and 18. The results show that all ENMs could be detected in A549 cells but the amounts varied between ENMs. On a qualitative basis, most intracellular ENMs were observed after treatment with CeO<sub>2</sub> NM-212, DQ12 and TiO<sub>2</sub> NM-105 followed by BaSO<sub>4</sub> NM-220. Only few ZnO NM-111 particles could be detected in A549 cells which could be attributed to the increased solubility of ZnO ENMs.

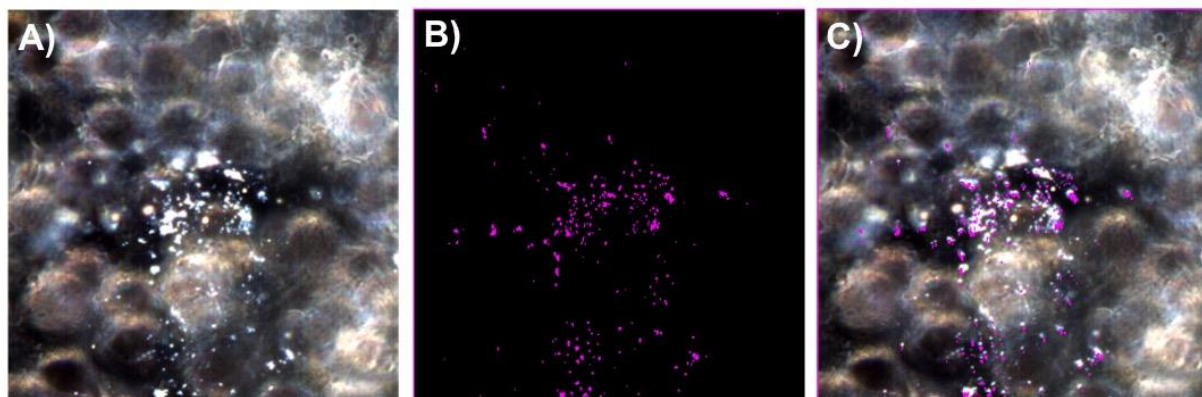


**Figure 17:** A) Darkfield image of CeO<sub>2</sub> particles (white) in A549 cells. B) The spectral angle map of the CeO<sub>2</sub> particles (purple). C) Overlay of darkfield image and spectral angle map.

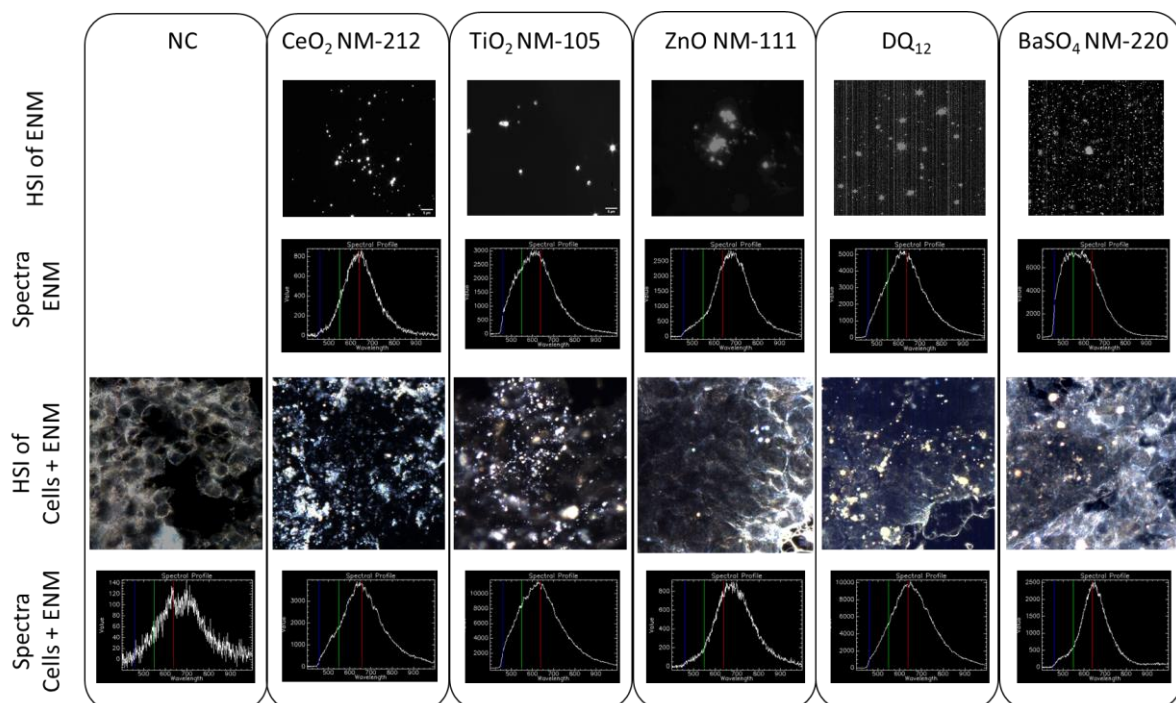


**Figure 18:** Hyperspectral images (HSI) of ENM particles only, of A549 epithelial cells treated with 100 µg/mL ENMs for 80 h (with arrows indicating intracellular ENM) and the corresponding spectra. NC: Negative control.

## 2.5 Fate of ENM in a 3D liver model (HWU, InSphere, NRCWE)

The fate of ENM in a 3D human liver microtissue model was assessed after long-term (3 weeks) repeated exposure to TiO<sub>2</sub> and CeO<sub>2</sub> nanomaterials. In summary, brightfield and enhanced darkfield imaging of cross-sections of microtissues exposed to TiO<sub>2</sub> and CeO<sub>2</sub> showed a concentration-dependent penetration of nanomaterials deep into the tissue (Fig. 19). Preliminary immunostaining indicated uptake of ENM by Kupffer cells. The experimental details and results will be reported in deliverable 4.2.

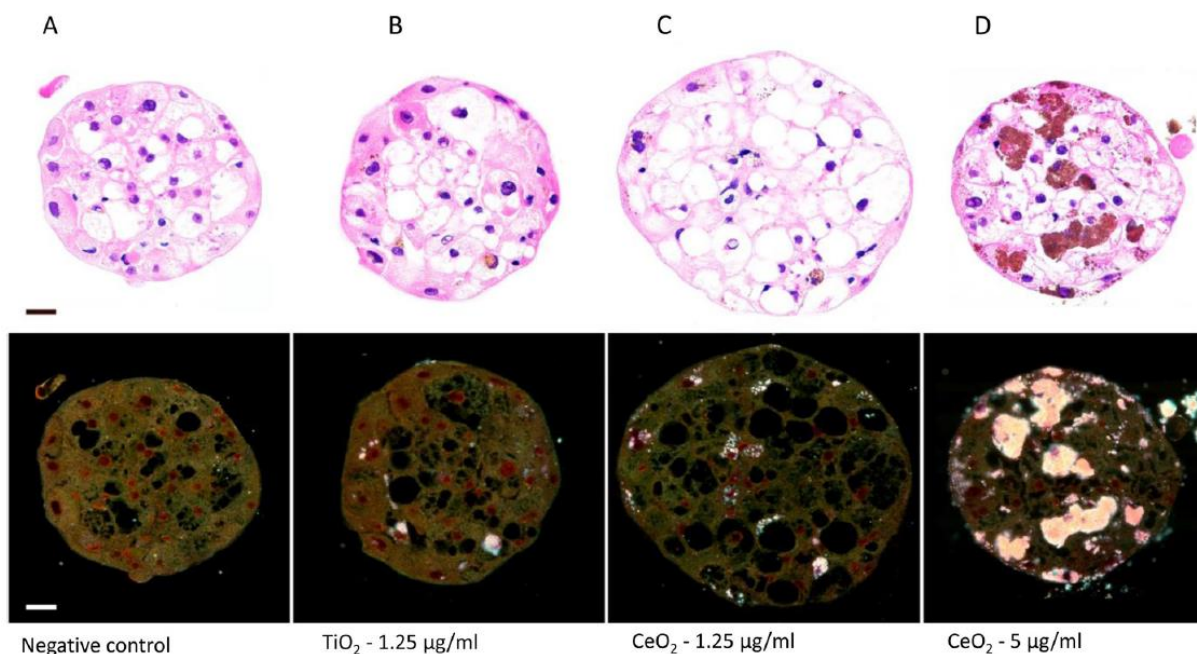


**Figure 19:** Representative brightfield and enhanced darkfield images of the distribution of ENMs in multi-cellular primary human liver microtissues after 3 weeks of cell culture. TiO<sub>2</sub> and CeO<sub>2</sub> appear brown in brightfield and white in darkfield. A: negative control, B: TiO<sub>2</sub> – 1.25 µg/ml, C: CeO<sub>2</sub> – 1.25 µg/ml and D: CeO<sub>2</sub> – 5 µg/ml. Haematoxylin and eosin-stained cross-sections. Scale bars 20 µm. *Kermanizadeh et al. 2019 Part Fibre Toxicol.*

## 2.6 Final conclusions

Understanding the fate of ENM in cells is of high relevance as a possible accumulation over repeated exposures might result in similar effects as upon exposure to high concentrations. In this task, we evaluated the different ENM fractions upon cell exposure using two complementary techniques, i.e. PIXE and ICP-OES. The PIXE technique was not able to produce data for all the conditions. However, the results suggest that most of the ENMs are retained in the cells and cellular membranes. The trends of the values obtained is comparable for both experiments, A549 and Caco-2 cells, with exception of the SiO<sub>2</sub> NM-200.

For the ICP-OES measurements, robust and reproducible data could be generated. We could demonstrate that the fate highly depends on the material properties such as size and solubility, in

addition, the exposure scenarios applied revealed interesting differences. If a high concentration is exposed to the cells, we could observe a decrease in the cellular fraction from 24 h to 80 h, possibly due to multifactorial behaviour involving cell division, cell loss, exocytosis or ions excretions. This might be different for cell systems where no cell division is happening.

In contrast, when cells were exposed repeatedly to low concentrations over 80h we measured an increase in the cellular fraction for all materials used, indicating indeed an accumulation, also in dividing cells. Finally, when we apply the same concentration once at a high concentration, and once repeatedly, a similar cellular fraction was detected showing that a repeated low-dose exposure leads to the same intracellular ENM burden as a single high dose after 80h.

### 3. Deviations from the Workplan

#### AMI:

Initial exposures of Tier1 materials were done using both Caco-2 as well as A549 cells. Quantification was done testing both ICP-OES as well as the PIXE technique. Due to technical problems using the PIXE technique and optimisation time for the ICP-OES technique, the main focus for the final studies was on A549 cells only.

#### UNamur:

XPS measurements, for the extreme surface composition determination, on samples from the A549 series were unsuccessful. The reason was that the LOD of the XPS at these nominal concentrations were low. Therefore, most of the analysis were performed with the PIXE technique. There was some significant delay in the measurements, mostly due to the difficulty on setting the correct conditions for the analysis, such as: establishing a protocol for the preparation of samples (dry or liquid), determining the adequate liquid volume for the analysis, settings and technical development for introducing the liquid sample under vacuum conditions). “Covid-19 lock-down” in the UNamur started on March the 16<sup>th</sup> and lasted till May the 4<sup>th</sup>. For this reason, we were not able to continue with the planned PIXE measurements (series in Caco-2 medium and completing series A549). For the same reason, we were not able to start with the  $\mu$ PIXE measurements (mapping of NPs in the vicinity of the cells).

#### USC / ISTE:

USC hosted a collaborator from ISTE, and her training for SP-ICP-MS was reported in D1.2. The deliverable activity from USC was then taken over by ISTE, providing quantification of the ENMs in the cell fractions by ICP-OES.

#### 4. Performance of the partners

All partners have formed a productive and collaborative approach within T1.4, with extensive discussion and support across partners to achieve the objectives of the task. There have been monthly TC's for this task, which has been based on sharing experimental data, methods and issues.

## 5. Conclusions

**The Steering Board deems this deliverable to be fulfilled satisfactorily for submission.**

**6. Annexes:**